Heliyon 7 (2021) e07485

Contents lists available at ScienceDirect

Heliyon

journal homepage: www.cell.com/heliyon

Research article

Ameliorating effect of melatonin on mercuric chloride-induced neurotoxicity in rats

Eman S. Said [a,b,*], Radwa M. Ahmed [c], Rehab A. Mohammed [d], Enas M. Morsi [e], Mohamed H. Elmahdi [f], Hassan S. Elsayed [g], Rania H. Mahmoud [g], Eman H. Nadwa [h,i]

[a] Department of Clinical Pharmacology, Faculty of Medicine, Fayoum University, Fayoum, Egypt
[b] Department of Pharmacology and Toxicology, College of Pharmacy, Qassim University, Saudi Arabia
[c] Department of Anatomy and Embryology, Faculty of Medicine, Fayoum University, Egypt
[d] Department of Medical Physiology, Faculty of Medicine, Fayoum University, Egypt
[e] Department of Forensic Medicine and Clinical Toxicology, Faculty of Medicine, Fayoum University, Egypt
[f] Department of Pathology, Faculty of Medicine, Fayoum University, Egypt
[g] Department of Medical Biochemistry and Molecular Biology, Faculty of Medicine, Fayoum University, Egypt
[h] Department of Pharmacology and Therapeutics, College of Medicine, Jouf University, Sakaka, Saudi Arabia
[i] Department of Medical Pharmacology, Faculty of Medicine, Cairo University, Giza, Egypt

HIGHLIGHTS

- $HgCl_2$ induced fragmentation of rough endoplasmic reticulum.
- Ballooning of Golgi apparatus.
- Nuclear and cytoplasmic degeneration of pyramidal neurons of rat cerebral cortex.
- $HgCl_2$ increased reactive oxygen species.
- Melatonin, free radical scavenger improved neuronal damage caused by $HgCl_2$.

ARTICLE INFO

Keywords:
Mercuric chloride
Melatonin
Cerebral cortex
Oxidative stress
Neurotoxicity

ABSTRACT

Mercury is a highly toxic metal. It induces its toxicity via production of reactive oxygen species. Brain tissues are more susceptible to oxidative damage. Melatonin and its metabolites are free radical scavengers. The aim of this work is to elucidate the neuroprotective effect of melatonin on mercuric chloride-induced neurotoxicity in rats. Fifty male albino rats were used and divided into five groups. Group I acts as normal control. Group II (LD $HgCl_2$) received mercuric chloride at a dose of 2 mg/kg. Group III (HD $HgCl_2$) received $HgCl_2$ at a dose of 4 mg/kg. Rats in group IV (LD $HgCl_2$ +MLT) received $HgCl_2$ 2 mg/kg + Melatonin 5 mg/kg. Rats in group V (HD $HgCl_2$+MLT) received $HgCl_2$ 4 mg/kg + Melatonin5 mg/kg. This study revealed that mercuric chloride decreased the activity of superoxide dismutase, catalase and glutathione peroxidase enzymes and increased malondialdehyde levels. Toxicity of mercuric chloride lead to upregulation of the gene expression level vascular endothelial growth factor. $HgCl_2$ induced fragmentation of rough endoplasmic reticulum, ballooning of Golgi apparatus, nuclear and cytoplasmic degeneration of pyramidal neurones of rat cerebral cortex. This neuronal damage caused by $HgCl_2$ was significantly improved by melatonin.

1. Introduction

Mercury is a highly toxic metal, present in the environment in three different forms: elemental, inorganic and organic. Inorganic mercury such as mercuric chloride has low lipid solubility so it is less absorbed and less passed through the blood brain barrier (BBB). Despite its poor ability to cross biological barriers, it is still able to induce motor deficits as it causes apoptosis and decreases number of neurons and astrocytes in

* Corresponding author.
E-mail addresses: Emanabdelmohti@gmail.com, e.abdelmoti@qu.edu.eg, ess02@fayoum.edu.eg (E.S. Said).

https://doi.org/10.1016/j.heliyon.2021.e07485
Received 14 February 2021; Received in revised form 18 May 2021; Accepted 1 July 2021

the motor cortex (Teixeira et al., 2018). Organic forms as methylmercury can cross BBB, accumulate in the hippocampus and damage its important function regarding learning and memory (Wu et al., 2016).

Accumulated mercury in sea foods represents the most widespread source for human consumption. Mercury is also used in numerous fields such as agriculture, Industry and medical field so its use cannot be avoided (Jha et al., 2019).

Organic and inorganic mercury are absorbed through the gastrointestinal tract and affect other systems via this route. Liver is the major site of metabolism of mercury and where it can accumulate leading to severe liver damage. Mercury can also cause nephrotoxicity, neurotoxicity, gastrointestinal toxicity and reproductive toxicity. The extent of damage possibly depends on both mercury concentration and the sensitivity of the organ (Oriquat et al., 2012; Rao et al., 2010).

Moreover, increased mercury exposure has been associated with coronary heart disease, hypertension and carotid artery atherosclerosis due to formation of reactive oxygen species (ROS) which are responsible for production of oxidized low density lipoprotein with subsequent atherosclerosis (Asgary et al., 2017; Rizzetti et al., 2016).

Many studies revealed that mercury induces its toxicity via production of ROS and rapid consumption of the protective antioxidant enzymes such as catalase, superoxide dismutase (SOD) and glutathione peroxidase (GSP) enzymes. ROS causes mitochondrial dysfunction, neuro inflammation, and apoptosis, overall resulting in neurodegenerative disorders and neuronal cell death. Accumulated mercury in the brain tissue increases the expression of N-methyl-D-aspartate (NMDA) receptors and enhances their responsiveness. Activation of NMDA type glutamate receptors stimulates Ca2+ entry into neurons, that leads to the motivation of pathways involved in neuronal cell death. Besides, Ca2+ stimulates ROS formation via the mitochondrial pathway (Jakaria et al., 2018; Jha et al., 2019; Rao et al., 2010).

Brain tissues are more liable to oxidative damage because of high concentration of polyunsaturated fatty acids that are predominantly susceptible to lipid peroxidation that plays a key role in necrosis and cell death (Teixeira et al., 2018).

Melatonin (N-acetyl-5-methoxy tryptamine) is one of the oldest molecules that can be traced back to the beginning of life. It is a neurohormone secreted from the pineal gland as well as extra-pineal sources as the gut and the skin, the retina, the testes, the ovary, the placenta, glial cells, and lymphocytes. It is highly lipophilic so it can cross the cellular and physiological barriers. Melatonin is found in all organisms and interacts with ROS that occurs during respiration, producing 3-hydroxymelatonin and other metabolites that are more radical scavengers than melatonin itself (Rocha et al., 2015; Zhao et al., 2019).

Melatonin is not a typical hormone since it acts through receptor-independent and receptor-dependent manners. The hormonal characteristics of melatonin are obvious in regulation of reproductive activity, help of sleep, upgrade of immune response, inhibition of carcinogenesis, elevation of stem cell production, anti-inflammatory activity and retarding some age-related problems. Some of these actions via binding of melatonin with cell membrane receptors, MT1 and MT2. Additionally, there are receptor-independent actions such as its free radical generating capacity, a unique action to cancer cells. The cytoplasmic enzyme quinone reductase 2 (QR2), designated as receptor MT3, has a detoxifying activity reducing melatonin oxidative damage (Bizzarri et al., 2013; Boutin, 2016; Zhao et al., 2019).

The present study elucidates the neuroprotective effect of melatonin on mercuric chloride-induced neurotoxicity with special attention to its antioxidant and anti-inflammatory effects.

2. Materials and methods

2.1. Ethical statement

The experimental protocol and all producers were approved by the Ethical Committee of Animal Care, Faculty of Medicine, Fayoum University, Fayoum, Egypt. Animals were treated according to guide for care and use of laboratory animal by national research council (Albus, 2012).

2.2. Drugs and chemicals

1. Mercuric chloride: Concentrations of 1 mg/ml and 0.5 mg/ml mercuric chloride (HgCl2) were prepared. The 1 mg/ml solution was prepared using 1 g of (HgCl2; Sigma–Aldrich Inc, USA) added to a solution of 998.5 ml of distilled water plus 1.5 ml of HNO3 (nitric acid). The 0.5 mg/ml solution was similarly prepared with 0.5 g of HgCl2 (Heath et al., 2009).

2. Melatonin: It was supplied in the form of 3 mg containing tablets (Nature's Bounty, USA), each tablet was dissolved in 5% ethanol.

2.3. Animals and housing

Fifty adult male albino rats of 180–220 g weight were used in this experiment. They were gotten from the animal house, Faculty of Medicine, Cairo University. Rats were delivered with a light-dark cycle of 12–12 h. The rats were housed in 5 cages according to their group at room temperature and provided with commercial laboratory food and free access to water.

2.4. Experimental design

Rats were subdivided into 5 groups (10 rats each).

Group 1: Normal control group: Rats were injected 0.5 ml distilled water intraperitoneally every other day and 1 ml distilled water by oral gavage daily for 60 days.

Group 2: Low dose mercuric chloride (LD HgCl2): Rats received mercuric chloride 2 mg/kg body weight by oral gavage daily for 60 days (Rao et al., 2010).

Group 3: High dose mercuric chloride (HD HgCl2): Rats of this group received mercuric chloride 4 mg/kg body weight by oral gavage daily for 60 days (Rao et al., 2010).

Group 4: Low dose mercuric chloride and melatonin (LD HgCl2+MLT): Rats of this group received mercuric chloride 2 mg/kg body weight by oral gavage daily for 60 days and melatonin 5 mg/kg body weight intraperitoneally every other day for 60 days, 25–30 min before the administration of mercuric chloride (Rao et al., 2010).

Group 5: High dose mercuric chloride and melatonin (HD HgCl2+MLT): Rats received mercuric chloride 4 mg/kg body weight by oral gavage daily for 60 days and melatonin as mentioned before.

- Because of the rapid metabolism of melatonin, it was administrated before HgCl2.

2.5. Sample collection

Animals were deeply anesthetized with ketamine hydrochloride (90 mg/kg) and xylazine hydrochloride (10 mg/kg) intraperitoneally. Rats were transcardially perfused with heparinized 0.9% saline solution. An incision was done at the posterior of the neck. The skull was removed carefully to expose the brain. Left and right hemispheres of the brain were dissected out (Aragão et al., 2018). Immediate fixation of right side of brain for 6 h in Bouin solution for brain sectioning and Immunohistochemical staining was performed. The left cerebral hemisphere was isolated and homogenates were prepared for further analysis of biochemical parameters.

2.6. Assay of oxidative stress levels

The levels of malondialdehyde (MDA) and glutathione peroxidase (GSP) were measured for analysis of lipid peroxidation. Additionally, superoxide dismutase (SOD) and catalase enzymes activities were investigated.

The sagittal sections of the cerebral tissue containing the cerebral motor cortex were homogenized using potassium phosphate buffer (50 mM, pH 7.4). The cerebral homogenates were divided into 2 subgroups. The first part was centrifuged at 4000 rpm for 15 min at 4 °C to collect the supernatant. Oxidative stress parameters were determined by commercially available kits (Biodiagnostic, Egypt), as previously described (El-Magd et al., 2017).

2.7. Quantitative real time PCR analysis

Total RNA was extracted from cerebral tissue homogenates of each group using QIAzol lysis reagent (miRNeasy Kits, Qiagen, USA). cDNA was prepared using reverse transcriptase kit, the Super Script III First-Strand Synthesis System as indicated by the manufacturer's protocol (Fermentas, USA). RT-PCR reactions were performed using TaqMan® gene expression assays for vascular endothelial growth factor (VEGF) and B-actin (Applied Biosystems). The primer sequences used were for VEGF: forward 5′- GGA CTT GAG TTG GGA GGA GGAT-3'; reverse 5′- CAG GGATGG GTT TGT CGT GTT-3′ and β-actin (as an internal control), forward 5′-ATC CGT AAA GAC CTC TAT GCC AAC A-3'; reverse 5′- GCTAGG AGC CAG GGC AGT AAT C-3'. Shortly, real-time RT-PCR was carried out in a25μl reaction volume consisting of QuantiTect SYBR Green PCR Master Mix, 2.5μl of each primer and 5μl of cDNA. Thermal cycling conditions were performed as follow: a pre-amplification step of 95 °C for 15 min, followed by amplification for 40 cycles of 94 °C for 15 s, 60 °C for 30 s, and 72 °C for 30 s. The expression of the VEGF gene mRNA was calculated using the threshold cycle method (ΔΔCT). The relative value for the control group was established as one (Mohammed et al., 2019).

2.8. Brain sectioning and immunohistochemical staining for glial fibrillary acidic protein (GFAP) in cerebral cortex

Following brain tissue samples were fixed in Bouin solution, they were immersed in paraplast (Monoject Scientific, Ireland). 7 μm thick sections were mounted in silanized slides. The sagittal sections containing the cerebral motor cortex were located just posterior to the coronal suture.

For immunohistochemical analysis, the slides were dewaxed in xylol and hydrated at increasing concentrations of ethanol. Buffering with citrate at pH 6.0 was done for antigenic recovery. Sections were treated with 0.2M boric acid (pH 9.0) at 65 °C for 25 min in order to enhance the labelling intensity. Treated sections were preserved at room temperature for 20 min and incubated in a 1% hydrogen peroxide solution to remove endogenous peroxidase, washed in phosphate buffered saline (PBS) and incubated with 2% bovine serum albumin (30 min) to remove non-specific background staining. Tissue sections were overnight incubated, at 4 °C with the following primary antibodies: mouse monoclonal antibodies for GFAP (1: 1000, Sigma, USA) as a marker for astrocytes activation. The sections then were washed in 0.05% PBS/Tween (Sigma Company, USA) solution three times for 5 min and incubated in goat serum in PBS for 1 h. After that, sections were rinsed in PBS/Tween solution for 5 min (3 times) and incubated with secondary antibodies, goat anti-rabbit IgG (Vector Laboratories, USA) diluted at 1: 500 in PBS for 2 h. We used normal serum rather than primary antibody in some sections as a negative control. Sections were washed again for three times, 5 min each, and incubated in the avidin-biotin-peroxidase complex (ABC Kit, Vector Laboratories, USA) for 2 h. Sections were rinsed four times, 5 min each, and revealed with diaminobenzidine (DAB) (to visualize the primary antibody binding sites). After the DAB reaction, sections were rinsed 2 times, 5 min each, in 0.1M PB (phosphate buffer pH 7.2), dehydrated, and cover-slipped (Aragão et al., 2018; Lima et al., 2016).

2.9. Quantitative morphometric study

- We made this morphometric study in the Pathology department, Faculty of Dentistry, Cairo University. Digitalized images were captured in four fields per section and five sections per animal using a graticule ($1mm^2$) attached to the eyepiece (objective 40x). Illustrative images from all experimental groups were obtained with a digital camera (Moticam 2500, USA) attached to a microscope (Nikon, Eclipse 50i, USA) and controlled by image analyzer software. The image analyzer was first calibrated automatically to convert the measurement units (pixels) produced by the image analyzer program into actual micrometer units.
- Area percent for GFAP immunohistochemical stained sections:

Sections from all groups were measured using an objective lens of magnification 40, a total magnification of 400 in non-overlapping fields.

2.10. Electron microscopic examination

The target area of study is: The sagittal sections containing the cerebral motor cortex:

Processing of sample:

A- Fixation: 1ry fixative: Glutaraldehyde (2.5%) 3–4 h, then wash with phosphate buffer saline (PBS) 0.1 M 10 min then overnight. Secondary fixative: Osmium Tetroxide (1%) 1.5 h, then wash with PBS twice 10 min each. A degradation of Ethanols for dehydration: 50% 10 min,70% 10 min, 95% 10 min and 100% 15 min 2 times.

B- Infiltration: propylene oxide (PO) 2 times 15 min each then a mixture of propylene oxide and epoxy resin: 1:2 (resin: po) 1 h in rotator, 1:1 (resin: po) overnight, 2:1 (resin: po) 4 h then change to 100% resin only overnight.

C- Embedding: in easy mold and place in oven overnight at 60 Celsius. By Ultramicrotome make a semi-thin section (500–1000 nm thickness) stained by Toluidine blue dye then observe under light microscope, followed by ultrathin sections (starting with 75nm and below 70, 65,…) placed on copper grids and stained with uranyl acetate and lead citrate.

Under Transmission Electron microscope (Jeol S 100, USA) (Chuang et al., 2009; Rybka et al., 2019).

2.11. Statistical analysis

The collected data was organized and statistically analysed using SPSS software statistical computer package version 22 (SPSS Inc., USA). The mean and standard deviation (SD) were calculated. One-way ANOVA was used to test the difference about mean values of measured variables between groups. Multiple comparisons between pairs of groups were performed using Tukey HSD (Post hoc range test). Significance was adopted at $P < 0.05$ for interpretation of results of tests of significance (Azzubaidi et al., 2013).

3. Results

In the present study as shown in Figure 1, mercuric chloride in both low and high doses significantly ($p < 0.05$) decreased the activities of SOD, catalase and GSP enzymes compared to control group. The mean ± SD of SOD in control, LD $HgCl_2$ and HD $HgCl_2$ groups was 7.11 ± 0.23, 5.89 ± 0.57 and 2.01 ± 0.65 respectively. Regarding catalase enzyme, the mean ± SD in control, LD $HgCl_2$ and HD $HgCl_2$ groups was 702.54 ± 66, 566.04 ± 44.02 and 234.08 ± 72.44 respectively while GSP levels were 77.55 ± 5.68, 51.67 ± 8.5 and 17.5 ± 7.13 respectively (Figure 1).

Melatonin improved this deficiency in enzymes activity. It significantly increased SOD, catalase and GSP levels in HD $HgCl_2$+MLT group compared to HD $HgCl_2$ group. The mean ± SD of SOD in HD $HgCl_2$ and HD $HgCl_2$+MLT groups was 2.01 ± 0.65 and 3.56 ± 0.49. Regarding catalase enzyme in HD $HgCl_2$ and HD $HgCl_2$+MLT groups was 234.08 ± 72.44 and 398.56 ± 13.13 while GSP was 17.5 ± 7.13 and 39.46 ± 5.19. The mean ± SD of SOD in LD $HgCl_2$ and LD $HgCl_2$+MLT groups was 5.89 ± 0.57 and 6.55 ± 0.20 respectively. Catalase enzyme in LD $HgCl_2$ and LD $HgCl_2$+MLT groups was 566.04 ± 44.02 and 681.41 ± 94.17.

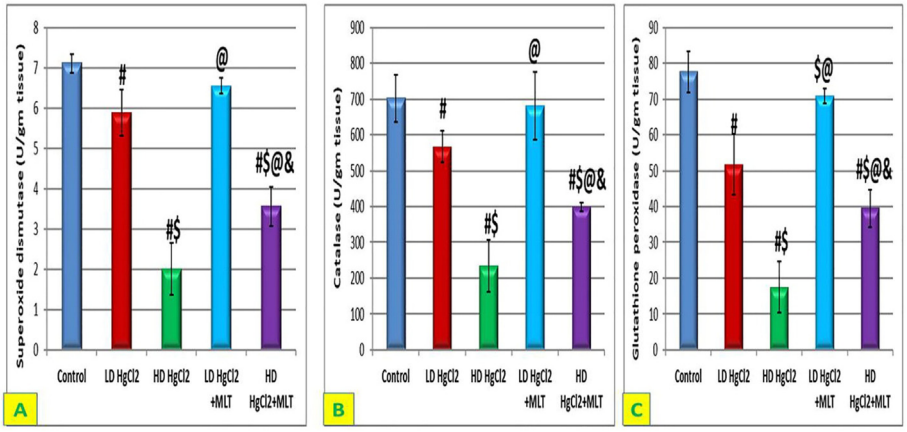

Figure 1. Effect of melatonin on SOD (A), catalase (B) and GSP (C) in brain tissue of mercuric chloride-induced neurotoxicity in rats. Values are expressed as mean ± SD, (n = 6). # is significant compared to control group. $ significant compared to LD HgCl2 group. @ significant compared to HD HgCl2 group. & significant compared to LD HgCl2+MLT group. Significant ($p < 0.05$).

Glutathione peroxidase was significantly higher in LD $HgCl_2$+MLT group (70.86 ± 2.05) compared to LD $HgCl_2$ (51.67 ± 8.5). There was insignificant difference between LD $HgCl_2$ and LD $HgCl_2$+MLT groups regarding SOD and catalase enzymes activity levels. Simultaneously there was noteworthy difference between HD HgCl2+MLT group compared to control group regarding the antioxidant activity. Moreover, there were comparable findings in LD $HgCl_2$+MLT and control group (Figure 1).

Mercuric chloride significantly increased MDA in HD $HgCl_2$ group compared to control group. Melatonin insignificantly decreased MDA either in LD $HgCl_2$+MLT or HD $HgCl_2$+MLT groups compared to LD $HgCl_2$ or HD $HgCl_2$ groups respectively. The mean ± SD of MDA in control, LD $HgCl_2$, HD $HgCl_2$, LD $HgCl_2$+MLT and HD $HgCl_2$+MLT groups was 0.14 ± 0.02, 0.32 ± 0.05, 2.02 ± 0.44, 0.19 ± 0.01 and 1.63 ± 0.48 respectively (Figure 2).

Mercuric chloride significantly ($p < 0.05$) increased vascular endothelial growth factor (VEGF) expression level by both low and high doses compared to control group. Melatonin significantly decreased VEGF in both LD $HgCl_2$+MLT and HD $HgCl_2$+MLT groups compared to LD $HgCl_2$ and HD $HgCl_2$ groups respectively. The mean ± SD of fold change levels of VEGF gene in control, LD $HgCl_2$, HD $HgCl_2$, LD $HgCl_2$+MLT and HD $HgCl_2$+MLT groups were 1.00 ± 0.41, 4.96 ± 0.94, 14.99 ± 2.28, 2.28 ± 0.49 and 7.68 ± 1.35 respectively. Interestingly, there was no significant difference regarding VEGF gene expression levels between LD $HgCl_2$+MLT and control groups (Figure 2).

Effects of chronic exposure to $HgCl_2$ on astrocyte density in the motor cortex of adult rats and examination of immune-stained sections (GFAP) induced cytotoxicity and apoptosis, evident by moderate positive reaction of GFAP; dark-brown astrocytes of different sizes in LD $HgCl_2$ group and weak positive reaction of GFAP; light-brown astrocytes of different sizes in HD $HgCl_2$ group compared to control animals that exhibited strong positive reaction of GFAP and dark-brown astrocytes. That means inorganic mercury causes neuronal cell death as shown in Figure 3. Melatonin administration improved this cytotoxicity and neuronal cell death as shown in Figure 4, group of LD $HgCl_2$+MLT showed strong positive reaction of GFAP; dark-brown astrocytes and group of HD $HgCl_2$+MLT presented week and moderate positive reaction of GFAP; light and dark-brown astrocytes.

GFAP area % was significantly lower in LD $HgCl_2$ and HD $HgCl_2$ groups compared to control group. Melatonin significantly increased GFAP area % in both LD $HgCl_2$+MLT and HD $HgCl_2$+MLT groups compared to LD $HgCl_2$ and HD $HgCl_2$ groups respectively. There was significant difference between HD $HgCl_2$+MLT and control group while LD $HgCl_2$+MLT was comparable to control. GFAP area % in control, LD $HgCl_2$, HD $HgCl_2$, LD $HgCl_2$+MLT and HD $HgCl_2$+MLT groups was 7.07 ± 1.45, 4.34 ± 0.69, 0.37 ± 0.2, 6.73 ± 0.78 and 2.56 ± 0.91respectively (Figure 5).

Electron microscopic examination results are demonstrated in Figures 6 and 7. Control group exhibited spherical to ovoid mitochondria (m) with intact cristae and rough endoplasmic reticulum (RER). The

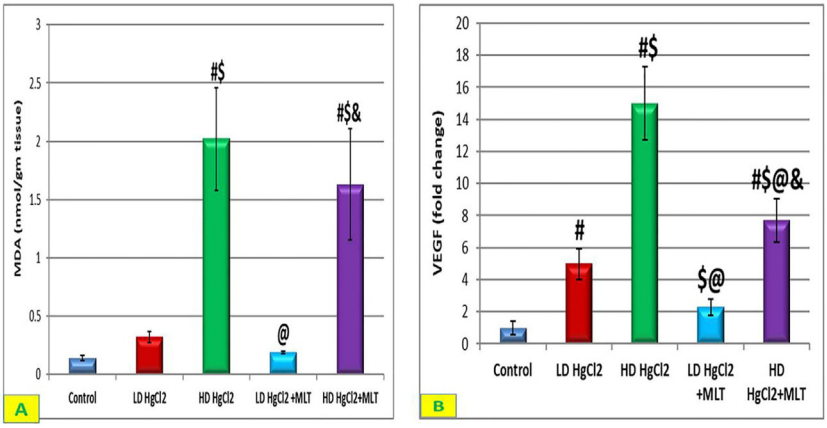

Figure 2. Effect of melatonin on MDA (A) and VEGF (B) in brain tissue of mercuric chloride-induced neurotoxicity in rats. Values are expressed as mean ± SD, (n = 6). # is significant compared to control group. $ significant compared to LD HgCl2 group. @ significant compared to HD HgCl2 group. & significant compared to LD HgCl2+MLT group. Significant ($p < 0.05$).

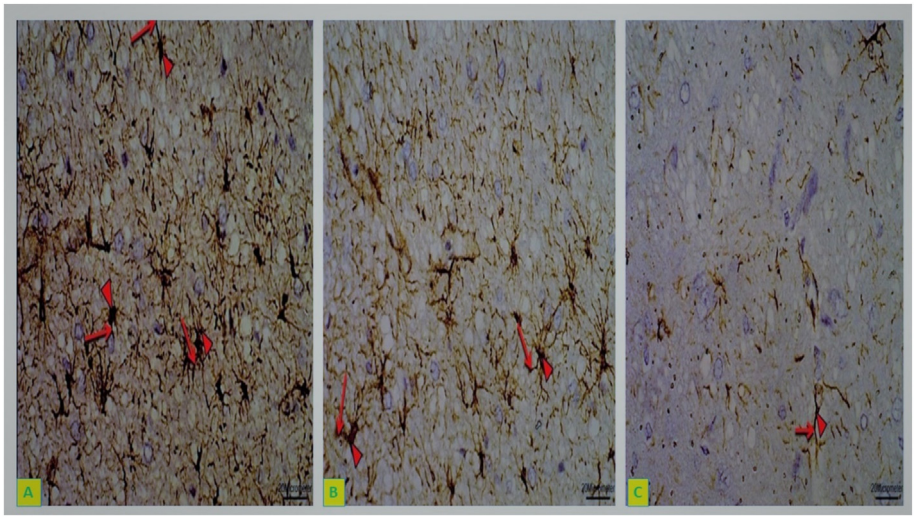

Figure 3. Effects of chronic exposure to HgCl2 on astrocyte density in the motor cortex of all groups. (A) represents photomicrograph of the GFAP-labelled motor cortex of control group, exhibiting strong positive reaction of GFAP; dark-brown astrocytes. LD HgCl2 group (B), showing moderate positive reaction of GFAP; dark-brown astrocytes. HD HgCl2 group (C), demonstrating week positive reaction of GFAP; light -brown astrocytes. Arrowheads represent brown astrocytes. Scale bar 20 μm.

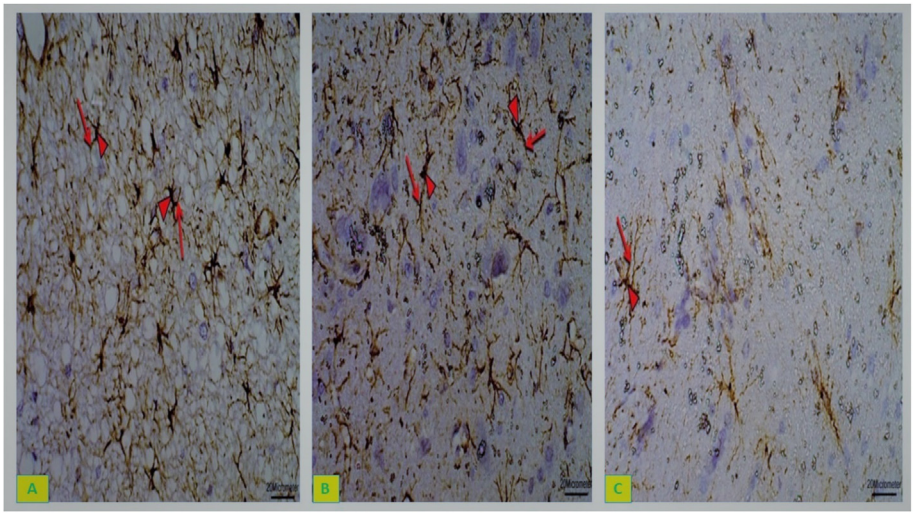

Figure 4. Effects of chronic exposure to HgCl2 on astrocyte density in the motor cortex of all groups. (A) represents photomicrograph of the GFAP-labelled motor cortex of LD HgCl2+MLT group, exhibiting strong positive reaction of GFAP; dark-brown astrocytes. (B&C) signifies HD HgCl2+MLT group, B exhibiting moderate positive reaction of GFAP; dark-brown astrocytes of different sizes with glial fibers & C showing week positive reaction of GFAP; light -brown astrocytes of different sizes with radial glial fibers. Arrowheads represent brown astrocytes. Scale bar 20 μm.

nucleus (N) is surrounded by bilaminar envelope with nuclear pores (arrowhead) and displays dispersed chromatin and evident nucleoli (n). Golgi apparatus can be observed (G) opposite nuclear pores. LD $HgCl_2$ group showed ballooned Golgi apparatus (G) opposite nuclear pores, fragmented forming cisterns with partially lost ribosomal surface RER, degenerated nucleus (N), with clumps of chromatin (chr) and blebbing of nuclear envelop (arrowhead). The mitochondria are either apparently normal with intact crisrae (m2) or ballooned with lost cristae (m1). HD $HgCl_2$ group revealed absent cytoplasmic organelles, extensive cytoplasmic rarefaction (R), extremely degenerated nucleus (N); karyolitic with clumped chromatin (chr) and indented nuclear envelope (arrowhead). LD $HgCl_2$+MLT group showed apparently normal nucleus (N) surrounded by bilaminar envelope with nuclear pores (arrowhead) and prominent nucleolus (n). Apparently normal Golgi apparatus can be observed (G) opposite nuclear pores and apparently normal RER can be observed. Most of mitochondria are apparently normal (m1) with intact cristae and few of them are ballooned with lost cristae (m2). HD $HgCl_2$+MLT group presented extensive cytoplasmic rarefaction (R), degenerated nucleus (N) with prominent nucleolus (n). Most of mitochondria are apparently normal (m) with intact cristae.

4. Discussion

The nervous system is one of the organs that are strongly affected by mercury toxicity leading to various neuropathologies and cognitive disabilities. Intense research on exact mechanisms of this toxicity revealed that its course and how to treat is still going on. The aim of the present work was to elucidate the neuroprotective effect of melatonin on mercuric chloride-induced neurotoxicity in rats.

In the present study, mercuric chloride in both low and high doses increased significantly the oxidative stress by decreasing antioxidants including SOD, catalase and GSP enzymes and increasing MDA compared to control group.

In agreement with the present work, a previous study investigating the role of vitamin E and Lactobacillus plantarum against mercuric chloride neurotoxicity. It concluded that mercuric chloride significantly diminished GSH level and SOD activity indicating increased oxidative stress (Fadda et al., 2020).

In another study, methyl mercury administration reduced non-enzymatic and enzymatic antioxidants such as SOD and GSP, that caused lipid, protein, and DNA oxidative damage and enhanced

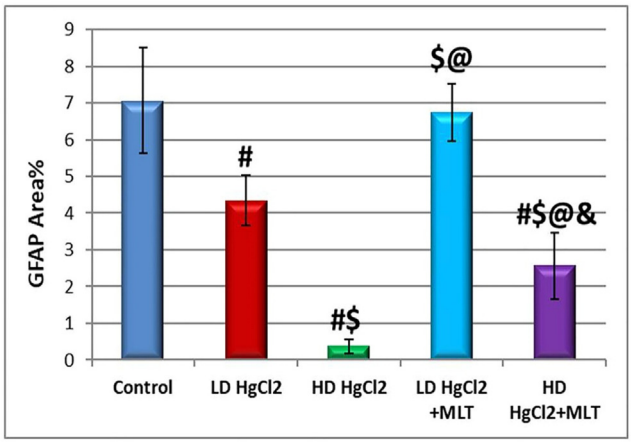

Figure 5. Histogram, illustrating area percent for GFAP distribution in the motor cortex in the different groups together with their statistical significance. Values are expressed as mean ± standard deviation, (n = 6). $ significant compared to LD HgCl2 group. @ significant compared to HD HgCl2 group. & significant compared to LD HgCl2+MLT group. Significant ($p < 0.05$).

neurocyte apoptosis in cerebral cortex (Liu et al., 2013). Additionally, the damage of cerebral neurones may occur by singlet oxygen, mostly due to oxidation of essential amino acids. Further, they found that heavy metals restrict lipid metabolism in the brain of animals and affect the metabolism of cholesterol, total lipids and triglycerides in the brain leading to imbalance between the lipids synthesis and breakdown. Mercuric chloride is believed to generate ROS in tissues and increasing MDA levels which indicating oxidation of unsaturated fatty acids in the brain with subsequent alteration in the anti-oxidative defence system both in experimental animals and humans (Omanwar and Fahim, 2015; Teixeira et al., 2018).

Also, supplementation with exogenous glutathione monoethyl ester protected against the methyl mercury augmented ROS formation and persuaded neuronal loss (Rush et al., 2012). Moreover, many studies determined increased oxidative stress induced by methyl mercury in which it caused oxidative damage by inducing GSH depletion, ROS production and inhibition of antioxidant enzyme activity (Deng et al., 2014).

In this work mercuric chloride increased VEGF expression. This cosistent with a previous study which demonstrated that over production of ROS by methyl mercury increased hypoxia inducible factor (HIF)-1α that upregulates transcription of VEGF that facilitates neuronal and blood brain barrier (BBB) damage via non-selective influx of cytotoxic agents and inflammatory cells from the blood into the brain tissue (Takahashi et al., 2017).

In the present study, marked decrease in GFAP-immuno reactive astrocytes has been observed in rat brain specimens treated with mercuric chloride that was evident especially with the use of high doses of mercury. These findings in agreement with an experimental study done on

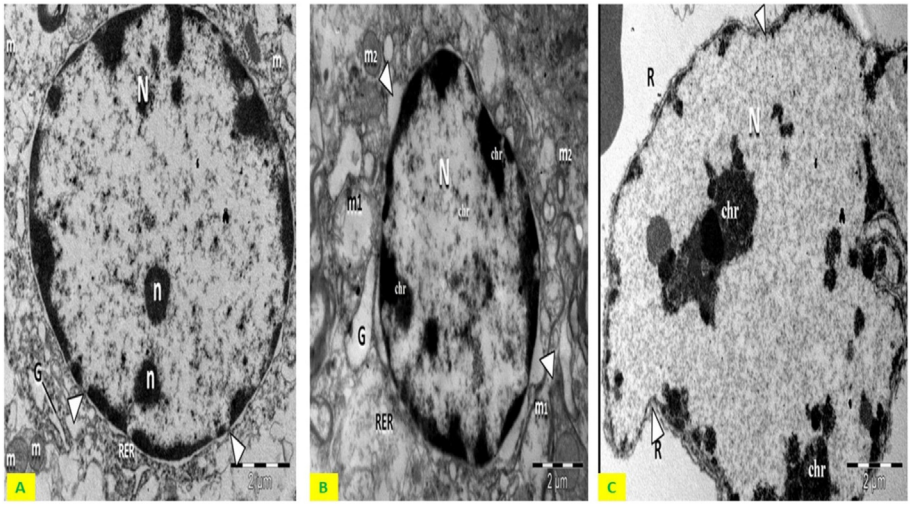

Figure 6. Ultragraph of control group (A), viewing spherical to ovoid (m) with intact cristae and (RER). (N) is surrounded by bilaminar envelope with nuclear pores (arrowhead) and displays dispersed chromatin and (n). (G) can be observed opposite nuclear pores. LD HgCl2 group (B), showing ballooned (G) opposite nuclear pores, fragmented RER forming cisterns with partially lost ribosomal surface, degenerated (N), with clumps of chromatin (chr) and blebbing of nuclear envelop (arrowhead). The mitochondria are either apparently normal with intact crisrae (m2) or ballooned with lost cristae (m1). HD HgCl2 group (C), displays absent cytoplasmic organelles, extensive cytoplasmic rarefaction (R), extremely degenerated nucleus (N); karyolitic with clumped chromatin (chr) and indented nuclear envelope (arrowhead). Mitochondria (m), rough endoplasmic reticulum (RER), the nucleus (N), an evident nucleoli (n) and Golgi apparatus (G). (EM x8900).

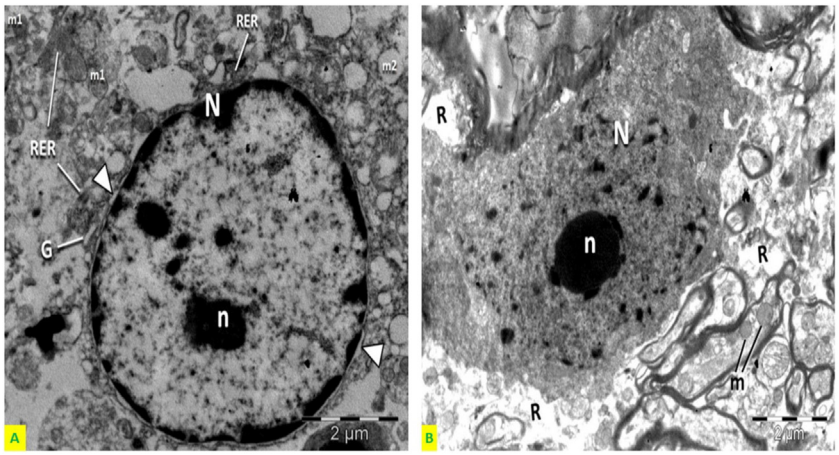

Figure 7. Ultragraph of LD HgCl2+MLT group (A), presenting apparently normal nucleus (N) surrounded by bilaminar envelope with nuclear pores (arrowhead) and prominent nucleolus (n). Apparently normal (G) can be observed opposite nuclear pores and apparently normal (RER) can be observed. Most of mitochondria are apparently normal (m1) with intact cristae and few of them are ballooned with lost cristae (m2). HD HgCl2+MLT group (B), showing extensive cytoplasmic rarefaction (R), degenerated nucleus (N) with prominent nucleolus (n). Most of mitochondria are apparently normal (m) with intact cristae. Mitochondria (m), rough endoplasmic reticulum (RER), the nucleus (N), an evident nucleoli (n) and Golgi apparatus (G). (EM x8900).

adult rats and found that chronic exposure to $HgCl_2$ even with very low dose induced cytotoxicity, apoptosis in the motor cortex and decreased the immunoreactivity of GFAP (Teixeira et al., 2018).

Similar to the present work, a previous study demonstrated that the neurotoxic effects of mercury chloride in rats were characterized by morphological changes for example neuronal loss, perivascular and pericellular edema with degeneration of astrocytes. These neuropathological changes accompanied by oxidative stress and increased lipid peroxidation which caused neuronal cell death (Jha et al., 2019).

Another study stated that the neurodegenerative disorders induced by mercuric chloride toxicity in mice in the form of ischemic neuronal injury with astroglia cells reaction, congestion, thrombosis and edema mainly in cerebrum, cerebellum and hippocampus (Ahmed, 2017).

In the current study, electron microscopic examination of rat brain specimens treated with mercuric chloride revealed nuclear and cytoplasmic degeneration, fragmented rough endoplasmic reticulum with lost ribosomal surface, ballooning of Golgi apparatus and mitochondria that lost their cristae. This was in agreement with Wu and his colleagues who found that rats infected with methyl mercury chloride showed damaged hippocampal ultrastructure in the form of abnormalities in dentate gyrus Golgi complex, endoplasmic reticulum and mitochondria with interstitial oedema (Wu et al., 2016).

In the present study, melatonin improved oxidative stress by significantly increasing SOD, catalase and GSP. Decreasing levels of MDA by melatonin in this study was insignificant. Regarding the antioxidant effect of melatonin, a number of studies in accordance with the present findings suggested the potential ability of melatonin to reverse the oxidative burden caused by different agents in different tissues. Ilbey and his colleagues induced state of oxidative stress in the renal tissue of male Wister albino rats using acetaminophen and they concluded that melatonin treatment reduced this oxidative load (Ilbey et al., 2009).

In another study investigated the antioxidant effect of melatonin using diquat to induce lipid peroxidation in rats stated that increase in liver enzymes while pre-treatment with melatonin reduced them indicating an antioxidant effect that was explained by the investigators as direct free radical scavenging ability and/or other antioxidative property induced by the indole (Zhang et al., 2006).

Moreover, a study group speculated the beneficial effect of melatonin on induced inflammation, oxidative stress and tissue repair in rats subjected to strenuous exercise evidenced by measurements of thiobarbituric acid reactive substances, activities of catalase, GSP, SOD, tumor necrosis factor-alpha, interleukin 1β, cytokine-induced neutrophil, l-selectin, macrophage inflammatory protein-3-alpha, and VEGF (Borges et al., 2015).

The Oxidant/antioxidant equilibrium has been pointed out in variable neurological diseases, of developmental, vascular, neoplastic, metabolic, immune, toxic and degenerative origins (Patel, 2016). In this context, the beneficial effect of melatonin as an antioxidant in brain injuries was tested by Zhao and his study group where they induced brain injury in mice by cecal ligation and puncture and compared the following for melatonin treated versus nontreated group; survival rate, BBB integrity, brain water content, levels of inflammatory cytokines (TNF-α and IL-1β), level of oxidative stress (SOD, catalase, and MDA), apoptosis and the expression of silent information regulator 1 (SIRT1). They reported that melatonin improved survival rate, attenuated brain oedema and neuronal apoptosis, preserved BBB integrity, decreased the production of TNF-α and IL-1β, increased the activity of SOD and CAT and decreased the MDA production. Additionally, melatonin upregulated the expression of SIRT1 suggesting that melatonin attenuates sepsis-induced brain injury via SIRT1 signalling activation (Zhao et al., 2015).

In another study questioning the potential neuroprotective role of melatonin in platinum-based chemotherapy, melatonin reversed manifestations of brain injury induced in rats by oxaliplatin, verified by improved neurobehavioral performances, locomotor activity, muscular strength, decreased hyperalgesia, altered inactivation of Bcl-2, caspase 3 apoptotic protein, Cytochrome c release and finally modulated altered non-enzymatic, enzymatic antioxidants and complex enzymes of mitochondria (Waseem et al., 2016).

Melatonin is not only a direct free radical scavenger, it also stimulates the synthesis of another important intracellular antioxidant, glutathione. It reduces electron leakage from the mitochondrial electron transport chain and has a synergistic effect with the other antioxidants (Hacışevki and Baba, 2018).

5. Conclusion

Mercuric chloride induced significant brain damage. This toxicity via production of reactive oxygen species as it decreased superoxide dismutase, catalase and GSP enzymes in addition to the increase in MDA and VEGF expression level. HgCl2 induced major neurodegenerative changes in the form of fragmentation of RER, ballooning of Golgi apparatus, nuclear and cytoplasmic degeneration of pyramidal neurons of rat cerebral cortex. This neuronal damage caused by HgCl2 was significantly improved by melatonin which is a free radical scavenger. The findings of the present study provide a rationale for testing the efficacy of melatonin as antioxidant and anti-inflammatory factor in the counties that have predominant mercury toxicity.

Declarations

Author contribution statement

Eman S. Said: Conceived and designed the experiments; Analyzed and interpreted the data; Contributed reagents, materials, analysis tools or data; Wrote the paper.

Radwa M. Ahmed: Conceived and designed the experiments.

Rehab A. Mohammed: Analyzed and interpreted the data.

Enas M. Morsi: Contributed reagents, materials, analysis tools or data.

Mohamed H. Elmahdi; Hassan S. Elsayed: Performed the experiments.

Rania H. Mahmoud: Performed the experiments and Analyzed and interpreted the data.

Eman H. Nadwa: Analyzed and interpreted the data; Wrote the paper.

Funding statement

This research did not receive any specific grant from funding agencies in the public, commercial, or not-for-profit sectors.

Data availability statement

Data will be made available on request.

Declaration of interests statement

The authors declare no conflict of interest.

Additional information

No additional information is available for this paper.

References

Ahmed, M.A.-Z., T, M.M.M., G, H., 2017. Neurodegenerative disorders associated with mercuric chloride toxicity in mice and the role of some antioxidant. Int. J. Sci. Res.(IJSR) 6, 1253–1260.

Albus, U., 2012. Guide for the Care and Use of Laboratory Animals, eighth ed. Laboratory Animals, pp. 267–268. 46.

Aragão, W.A.B., Teixeira, F.B., Fagundes, N.C.F., Fernandes, R.M., Fernandes, L.M.P., Da Silva, M.C.F., Amado, L.L., Sagica, F.E.S., Oliveira, E.H.C., Crespo-Lopez, M.E., Maia, C.S.F., Lima, R.R., 2018. Hippocampal dysfunction provoked by mercury chloride exposure: evaluation of cognitive impairment, oxidative stress, tissue injury and nature of cell death. Oxid. Med. Cell. Longev. 2018.

Asgary, S., Movahedian, A., Keshvari, M., Taleghani, M., Sahebkar, A., Sarrafzadegan, N., 2017. Serum levels of lead, mercury and cadmium in relation to coronary artery disease in the elderly: a cross-sectional study. Chemosphere 540–544.

Azzubaidi, M.S., Saxena, A.K., Talib, N.A., 2013. Quantifying ca1 dorsal hippocampal pyramidal cells in rats: rules to light microscope based estimation. Malays. J. Microscop. 9, 165–169.
Bizzarri, M., Proietti, S., Cucina, A., Reiter, R.J., 2013. Molecular mechanisms of the pro-apoptotic actions of melatonin in cancer: a review. Expert Opin. Therap. Targ. 1483–1496.
Borges, L.D.S., Dermargos, A., Junior, E.P.D.S., Weimann, E., Lambertucci, R.H., Hatanaka, E., 2015. Melatonin decreases muscular oxidative stress and inflammation induced by strenuous exercise and stimulates growth factor synthesis. J. Pin. Res. 58, 166–172.
Boutin, J.A., 2016. Quinone reductase 2 as a promising target of melatonin therapeutic actions. Expert Opin. Therap. Targ. 303–317.
Chuang, Y.C., Lin, J.W., Chen, S. Der, Lin, T.K., Liou, C.W., Lu, C.H., Chang, W.N., 2009. Preservation of mitochondrial integrity and energy metabolism during experimental status epilepticus leads to neuronal apoptotic cell death in the hippocampus of the rat. Seizure 18, 420–428.
Deng, Y., Xu, Z., Xu, B., Liu, W., Wei, Y., Li, Y., Feng, S., Yang, T., 2014. Exploring cross-talk between oxidative damage and excitotoxicity and the effects of riluzole in the rat cortex after exposure to methylmercury. Neurotoxic. Res. 26, 40–51.
El-Magd, M.A., Abdo, W.S., El-Maddaway, M., Nasr, N.M., Gaber, R.A., El-Shetry, E.S., Saleh, A.A., Alzahrani, F.A.A., Abdelhady, D.H., 2017. High doses of S-methylcysteine cause hypoxia-induced cardiomyocyte apoptosis accompanied by engulfment of mitochondaria by nucleus. Biomed. Pharmacother. 94, 589–597.
Fadda, L.M., Alhusaini, A.M., Hasan, I.H., Ali, H.M., Al-Qahtani, Q.H., Zakaria, E.A., Alanazi, A., 2020. Combination of vitamin E and Lactobacillius plantarum reverses mercuric chloride-induced neurotoxicity: implication of BDNF, CREB and MAPK proteins expressions. J. King Saud Univ. Sci. 32, 2590–2597.
Hacıșevki, A., Baba, B., 2018. An overview of melatonin as an antioxidant molecule: a biochemical approach. In: Melatonin - Molecular Biology, Clinical and Pharmaceutical Approaches, pp. 59–85.
Heath, J.C., Abdelmageed, Y., Braden, T.D., Nichols, A.C., Steffy, D.A., 2009. The effects of chronic mercuric chloride ingestion in female Sprague-Dawley rats on fertility and reproduction. Food Chem. Toxicol. 47, 1600–1605.
Ilbey, Y.Ö., Ozbek, E., Cekmen, M., Somay, A., Ozcan, L., Otünctemur, A., Simsek, A., Mete, F., 2009. Melatonin prevents acetaminophen-induced nephrotoxicity in rats. Int. Urol. Nephrol. 41, 695–702.
Jakaria, M., Park, S.Y., Haque, M.E., Karthivashan, G., Kim, I.S., Ganesan, P., Choi, D.K., 2018. Neurotoxic agent-induced injury in neurodegenerative disease model: focus on involvement of glutamate receptors. Front. Mol. Neurosci. 11, 1–20.
Jha, A., Saidullah, B., Bubber, P., 2019. A study on prooxidative and neurotoxic effects of mercury chloride in rats. EC Pharmacol. Toxicol. 7, 175–187.
Lima, R.R., Santana, L.N.S., Fernandes, R.M., Nascimento, E.M., Oliveira, A.C.A., Fernandes, L.M.P., Santos, E.M.N.D., Tavares, P.A.N., Santos Dos, I.R., Gimarães-Santos, A., Gomes-Leal, W., 2016. Neurodegeneration and glial response after acute striatal stroke: histological basis for neuroprotective studies. Oxid. Med. Cell. Long. 2016.
Liu, W., Xu, Z., Deng, Y., Xu, B., Wei, Y., Yang, T., 2013. Protective effects of memantine against methylmercury-induced glutamate dyshomeostasis and oxidative stress in rat cerebral cortex. Neurotoxic. Res. 24, 320–337.
Mohammed, M.A., Aboulhoda, B.E., Mahmoud, R.H., 2019. Vitamin D attenuates gentamicin-induced acute renal damage via prevention of oxidative stress and DNA damage. Hum. Experim. Toxicol. 38, 321–335.
Omanwar, S., Fahim, M., 2015. Mercury exposure and endothelial dysfunction: an interplay between nitric oxide and oxidative stress. Int. J. Toxicol. 34, 300–307.
Oriquat, G.A., Saleem, T.H., Naik, R.R., Moussa, S.Z., Al-gindy, R.M., 2012. A Sub-chronic Toxicity Study of Mercuric Chloride in the Rat, pp. 141–146, 5.
Patel, M., 2016. Targeting oxidative stress in central nervous system disorders. Trends Pharmacolog. Sci. 37, 768–778.
Rao, M.V., Purohit, A., Patel, T., 2010. Melatonin protection on mercury-exerted brain toxicity in the rat. Drug Chem. Toxicol. 33, 209–216.
Rizzetti, D.A., Altermann, C.D.C., Martinez, C.S., Peçanha, F.M., Vassallo, D.V., Uranga-Ocio, J.A., Castro, M.M., Wiggers, G.A., Mello-Carpes, P.B., 2016. Ameliorative effects of egg white hydrolysate on recognition memory impairments associated with chronic exposure to low mercury concentration. Neurochem. Int. 101, 30–37.
Rocha, C.S., Rato, L., Martins, A.D., Alves, M.G., Oliveira, P.F., 2015. Melatonin and male reproductive health: relevance of darkness and antioxidant properties. Current Molecular Medicine 15, 299–311.
Rush, T., Liu, X., Nowakowski, A.B., Petering, D.H., Lobner, D., 2012. Glutathione-mediated neuroprotection against methylmercury neurotoxicity in cortical culture is dependent on MRP1. NeuroToxicology 33, 476–481.
Rybka, V., Suzuki, Y.J., Gavrish, A.S., Dibrova, V.A., Gychka, S.G., Shults, N.V., 2019. Transmission electron microscopy study of mitochondria in aging brain synapses. Antioxidants 8 (6), 171.
Takahashi, T., Fujimura, M., Koyama, M., Kanazawa, M., Usuki, F., Nishizawa, M., Shimohata, T., 2017. Methylmercury causes blood-brain barrier damage in rats via upregulation of vascular endothelial growth factor expression. PLoS ONE 12, 1–10.
Teixeira, F.B., de Oliveira, A.C.A., Leão, L.K.R., Fagundes, N.C.F., Fernandes, R.M., Fernandes, L.M.P., da Silva, M.C.F., Amado, L.L., Sagica, F.E.S., de Oliveira, E.H.C., Crespo-Lopez, M.E., Maia, C.S.F., Lima, R.R., 2018. Exposure to inorganic mercury causes oxidative stress, cell death, and functional deficits in the motor cortex. Front. Mol. Neurosci. 11, 1–11.
Waseem, M., Tabassum, H., Parvez, S., 2016. Neuroprotective effects of melatonin as evidenced by abrogation of oxaliplatin induced behavioral alterations, mitochondrial dysfunction and neurotoxicity in rat brain. Mitochondrion 30, 168–176.
Wu, J., Cheng, G., Lu, Z., Wang, M., Tian, J., Bi, Y., 2016. Effects of methyl mercury chloride on rat Hippocampus structure. Biolog. Trace Elem. Res. 171, 124–130.
Zhang, L., Wei, W., Xu, J., Min, F., Wang, L., Wang, X., Cao, S., Tan, D.X., Qi, W., Reiter, R.J., 2006. Inhibitory effect of melatonin on diquat-induced lipid peroxidation in vivo as assessed by the measurement of F2-isoprostanes. Journal of Pineal Research 40, 326–331.
Zhao, D., Yu, Y., Shen, Y., Liu, Q., Zhao, Z., Sharma, R., Reiter, R.J., 2019. Melatonin synthesis and function: evolutionary history in animals and plants. Front. Endocrinol. 10, 1–16.
Zhao, L., An, R., Yang, Y., Yang, X., Liu, H., Yue, L., Li, X., Lin, Y., Reiter, R.J., Qu, Y., 2015. Melatonin alleviates brain injury in mice subjected to cecal ligation and puncture via attenuating inflammation, apoptosis, and oxidative stress: the role of SIRT1 signaling. J. Pin. Res. 59, 230–239.